HHS Public Access

Author manuscript

Nature. Author manuscript; available in PMC 2009 November 30.

Published in final edited form as:

Nature. 2009 April 23; 458(7241): 1034–1038. doi:10.1038/nature07831.

Glycerol monolaurate prevents mucosal SIV transmission

Qingsheng Li[1], **Jacob D. Estes**[2], **Patrick M. Schlievert**[1], **Lijie Duan**[1], **Amanda J. Brosnahan**[1], **Peter J. Southern**[1], **Cavan S. Reilly**[3], **Marnie L. Peterson**[4], **Nancy Schultz-Darken**[5], **Kevin G. Brunner**[5], **Karla R. Nephew**[5], **Stefan Pambuccian**[6], **Jeffrey D. Lifson**[2], **John V. Carlis**[7], and **Ashley T. Haase**[1]

[1] Department of Microbiology, Medical School, University of Minnesota, MMC 196, 420 Delaware Street S.E., Minneapolis, Minnesota 55455, USA

[2] AIDS and Cancer Virus Program, Science Applications International Corporation–Frederick, Inc., National Cancer Institute, Frederick, Maryland, USA

[3] Division of Biostatistics, School of Public Health, University of Minnesota, MMC 303, 420 Delaware Street S.E., Minneapolis, Minnesota 55455, USA

[4] Department of Experimental and Clinical Pharmacology, College of Pharmacy, University of Minnesota, 2001 6th Street S.E., Minneapolis, Minnesota 55455, USA

[5] Wisconsin National Primate Research Center, University of Wisconsin, 1220 Capitol Court, Madison, Wisconsin 53715, USA

[6] Department of Laboratory Medicine and Pathology, Medical School, University of Minnesota, MMC 76, 420 Delaware Street S.E., Minneapolis, Minnesota 55455, USA

[7] Department of Computer Science and Engineering, Institute of Technology, University of Minnesota, 200 Union Street S.E., Minneapolis, Minnesota 55455, USA

Abstract

While there has been great progress in treating HIV-1 infection1, preventing transmission has thus far proven an elusive goal. Indeed, recent trials of a candidate vaccine and microbicide have been disappointing, both for want of efficacy and concerns about increased rates of transmission2–4. Nonetheless, studies of vaginal transmission in the SIV-rhesus macaque model point to opportunities in the earliest stages of infection where a vaccine or microbicide might be protective, by limiting the expansion of infected founder populations at the portal of entry5, 6. Here we show in this SIV-macaque model, that an outside-in endocervical mucosal signalling system, involving MIP-3α, plasmacytoid dendritic cells and CCR5+cell-attracting chemokines produced by these cells, in combination with the innate immune and inflammatory responses to infection in both cervix and vagina, recruit CD4+T cells to fuel this obligate expansion. We then show that glycerol monolaurate, a widely used antimicrobial compound 7 with inhibitory activity against production

Correspondence should be addressed to A.T.H. (haase001@umn.edu).

COMPETING INTERESTS STATEMENT

The authors declare that they have no competing financial interests.

of MIP-3α and other proinflammatory cytokines8, can inhibit mucosal signalling and the innate and inflammatory response to HIV-1 and SIV *in vitro*, and *in vivo* can protect rhesus macaques from acute infection despite repeated intra-vaginal exposure to high doses of SIV. This novel approach, plausibly linked to interfering with innate host responses that recruit the target cells necessary to establish systemic infection, opens a promising new avenue for development of effective interventions to block HIV-1 mucosal transmission.

To understand how SIV infection in a small founder population of cells at the portal of entry transitions in less than two weeks to systemic infection, with massive levels of viral replication and depletion of gut CD4+T cells 5, 6, 9, 10, we analyzed the anatomic and temporal expansion of these small founder populations. We created atlases of the numbers and locations of SIV RNA+cells detected by *in situ* hybridization in cervical vaginal tissues from animals at 4–10 days post-inoculation (dpi), with the rationale, that by locating sites that initially had the largest numbers of infected cells, and then determining how infection expanded and spread from these infected founder populations, we would gain insight into sites of virus entry and subsequent events underlying the expansion on which systemic infection depends.

In screening 20–40 sections of cervical vaginal tissues from each animal in this 4–10 dpi time frame, we identified sections with SIV RNA+cells in 9 animals, and in each animal found one predominant focus of infected cells in the endocervix. There were additional clusters of infected cells in the transformation zone (junction of ecto- and endocervix) adjoining the endocervical and vaginal foci in three animals. We illustrate at the bottom of Figure 1a the thumbnail images representative of the montages created from the captured images of sections from these animals, and in Figure 1b a small cluster of SIV RNA+cells found at 4 dpi only in endocervix, and then in one of forty sections in one isolated area, as reported previously6. We mapped onto a two-dimensional grid the positions of cell centers (centroids) of SIV RNA+cells in this focus (Figure 1c), and predominant foci at 6 to 10 dpi that were again found in endocervix.

These atlases revealed that infection expands by accretion of new infections around an initial cluster of infected cells in endocervix, rather than by diffuse spread of infection in the submucosa, and that successive influxes of new CD4+T target cells in inflammatory infiltrates fuels local expansion. The dramatic growth of SIV RNA+clusters is evident from comparisons of the map dimensions from 4 to 10 dpi (Figure 1d and e and Supplemental Figure 1a–c), and the growth of clusters amidst inflammatory cell infiltrates illustrated in Figure 1f at 6 dpi, where SIV RNA+cells are located amidst dark staining nuclei of cells in inflammatory infiltrates. These focal infiltrates contained increased numbers of CD4+T cells compared to uninfected animals, or at 1 dpi, and were apparent at 4 dpi (Figure 2a–c and Supplemental Figure 2). Virtually all of the infected cells were CD3+CD4+T cells (Figure 2d).

The isolated focus at 4 dpi seemed unlikely by itself to have induced such an extensive influx of CD4+T cells, and indeed we found evidence implicating endocervical epithelium and plasmacytoid dendritic cells (pDCs) in initially recruiting target cells to the endocervical submucosa. We had previously stained these tissues for a pDC marker 11, CD123, in

investigating the possible role of pDCs in a “premature” T regulatory response to infection12, and now noted areas with CD123+pDCs aligned just beneath the endocervical epithelium. These subepithelial pDC collections were observed 1 dpi, and were not seen in the same numbers or location in uninfected animals (Figure 3a–c). The pDCs also stained with the specific marker BDCA211 (not shown), were strongly positive for interferons α (Figure 3d) and β (not shown), and expressed the CCR5+cell-attracting chemokines MIP-1α and MIP-1β (Figure 3e), which could thus serve as one mechanism to quickly recruit CD4+T cells to the endocervix. We also found increased expression at 1 and 3 dpi of cervical MIP-3α/CCL20, the principal chemokine known to induce pDC migration and T cells into peripheral issues13, in microarray comparisons (Supplemental Table 1) of uninfected and infected animals, and increased MIP-3α/CCL20 staining in endocervical epithelium (Figure 3f). These findings reveal an outside-in signalling pathway triggered by exposure to the viral inoculum that recruits pDCs and T cells to create an environment rich in target cells at the sites of initial infection.

This initial influx of CD4+T cells was followed by a secondary inflammatory process, likely driven by RANTES and other chemokine- producing cells within inflammatory infiltrates (Supplemental Figure 3) in which SIV RNA+cells were clearly concentrated at 10dpi (Supplemental Figure 1d). Unlike endocervix, we saw no evidence of a signaling pathway capable of recruiting additional CD4+T cells in the foci of SIV RNA+cells in the transformation zone and vagina in three animals. However, an inflammatory response provided susceptible target cells for expansion of the infection at these sites as well, because infected cells (Supplemental Figure 4a), were generally in areas of inflammation containing IL-8+cells, with associated epithelial thinning and disruption (Supplemental Figure 4b–c). Thus, inflammation with increases in susceptible target populations is the common denominator across sites.

The importance of the innate immune and inflammatory response in providing new target cells for local expansion and systemic dissemination suggested that inhibiting this immunoinflammatory process might prevent transmission and systemic infection. We focussed on glycerol monolaurate (GML), because of the compound’s documented relevant activities in inhibiting immune activation and chemokine and cytokine production by human vaginal epithelial cell cultures (HVECs) on exposure to staphylococcal toxins8, 14. We showed that GML inhibited production of MIP-3α/CCL20 and IL-8 (as a general marker of inflammation and increased susceptibility to HIV-1 infection in female genital tissues 15) by HVECs in response to the more relevant exposure to HIV-1 (Figure 4a and b), and reduced MIP-3α/IL-8 levels (Figure 4c) in cervical vaginal fluids collected in a safety study16 from rhesus macaques treated intra-vaginally daily for six months with 5% GML.

Encouraged by these results, we tested GML’s potential efficacy against repeated high dose intra-vaginal SIV challenges in 10 animals, in an extension of the GML safety study16. We first evaluated GML’s efficacy in a pilot study in which we could examine cervical vaginal and lymphatic tissues obtained at the expected peak of viral replication at 14 dpi6. Two animals from the safety study that were treated daily with 5% GML in K-Y warming gel and two animals that had received just K-Y warming gel, as a vehicle control, were challenged intra-vaginally one hour after compound introduction with 10^5 $TCID_{50}$ of SIV. Four hours

later, they were again given either GML or K-Y warming gel, and challenged one hour later with an equivalent dose of SIV, and then continued on daily GML or K-Y warming gel.

Both GML-treated animals were completely protected from this high dose challenge. There was no evidence by *in situ* hybridization for SIV RNA+cells in cervical vaginal (Supplemental Figure 5a, b) or lymphatic tissues (not shown), and no evidence of inflammation (Supplemental Figure 5a, b) or virus detectable in plasma (Figure 5a). By contrast, in one of the two controls, SIV RNA+ cells were detected in endocervical, vaginal (Supplemental Figure 5c, d) and lymphatic tissues (not shown) and an influx of inflammatory cells associated with infection in the endocervix and vagina (Supplemental Figure 5c, d), and high levels of virus in plasma (Figure 5a) were all readily apparent. We then challenged three additional GML-treated animals and three K-Y warming gel controls, repeating the challenges 4 weeks later if the animals showed no evidence of systemic infection (plasma levels of < 20 copies of SIV RNA/ml). Again, GML prevented acute systemic infection after four exposures to this high dose vaginal challenge, whereas all three-control animals became infected (Figure 5b).

In seeking interventions to prevent vaginal transmission in a SIV-macaque model, we have focused on that critical window of opportunity in the earliest stages of infection when infected founder populations are small, and virus must overcome the limited availability of susceptible target cells to sustain and sufficiently expand the initially infected founder cell populations to disseminate and establish a self-propagating infection in secondary lymphoid organs5. We show here that SIV exploits the innate immune and inflammatory response to overcome this inherent limitation in the availability of target cells in the endocervix, the predominant site where of the initial infected cell clusters. We document the growth of clusters by accretion of new infections in influxes of CD4+T cell targets, and provide evidence plausibly linking the first influx to an outside-in mucosal signalling pathway in which exposure of endocervical epithelium to the viral inoculum increases expression of MIP3-α to recruit pDCs, which, in turn produce MIP-1α and MIP-1β to recruit CCR5+targets.

The discovery reported here of *in vivo* induction of MIP3-α in endocervical epithelium, together with *in vitro* results here and report of induction of MIP3-α in uterine epithelial culturesby microbial-related stimuli 17, point to outside-in signalling as a general feature of mucosal epithelium of the upper female genital tract. This signalling pathway and the evidence of production of interferons and virus-inhibiting chemokines by pDCs, support the concept that the mucosal lining of the upper female genital tract is truly the front line of the innate mucosal immune system18. While our conclusion, that innate defenses there are actually critical to the establishment and spread of infection, may thus at first seem counter intuitive, that conclusion is in keeping with report of possibly-enhanced vaginal transmission with agonists used to stimulate innate immunity19, and with the concept advanced here: while interferons and anti-viral chemokines locally produced by pDCs may protect themselves and contribute to limiting infection initially, *on balance*, SIV's greater immediate need is for target cells, which is served by the inflammatory component of the innate immune response.

We show that GML can break this vicious cycle of signalling and inflammatory responses in cervix and vagina to prevent acute SIV infection in five of five animals with repeated intra-vaginal challenges of 10^5 $TCID_{50}$ of SIV, and, particularly impressively, in three of three animals challenged four times with this high dose. This result represents a novel and highly encouraging new lead in the search for an effective microbicide to prevent HIV-1 transmission that meets the criteria of safety, affordability and efficacy 20. GML is a US Federal Drug Administration (FDA) -generally recognized as safe (GRAS) 7 agent that has been daily-applied intra-vaginally in K-Y warming gel, an FDA-approved vehicle for human vaginal use, for 6 months in rhesus macaques with no evidence of pathological effects or alteration of resident *Lactobacilli* 16. GML is inexpensive (each dose used here cost less than one cent), and is efficacious in preventing acute systemic infection.. Certainly, longer-term and well-powered studies with larger numbers of animals will be needed to definitively establish efficacy, and efficacy against occult infections, reportedly manifest as long as a year following repeated low-dose intravaginal inoculations21, and for which we now have preliminary evidence in this repeated high-dose model in one of the three animals with previously undetectable virus. Even conservative estimates of efficacy ≥ 60 percent (see statistical methods) extrapolate, according to mathematical models, to 2.5 million averted HIV infections over a 3- year period22, thus providing rationale and motivation for human trials of GML alone as a microbicide, and/or combined with other agents that specifically inhibit HIV-1 replication23. More generally, other microbes may exploit mucosal signalling and the innate inflammatory response to establish infection, so that GML may be the first example of a class of compounds that provide protection through interfering with these responses.

Methods Summary

Animals, inoculation of SIV, GML and K-Y warming gel

Adult female rhesus macaque monkeys (*Macacca mulatta*), housed in accordance with the regulations of the American Association of Accreditation of Laboratory Animal Care standards, were inoculated twice intra-vaginally with one ml of 10^5 $TCID_{50}$/ml SIVmac 2516. One ml K-Y warming gel ± 5% GML was administered atraumatically into the vagina daily and before viral challenges.

SIV RNA in plasma

SIV RNA copy Eq/ml in plasma was determined using a quantitative reverse-transcription PCR assay24.

In situ hybridization and immunohistochemistry

Blood, cervical-vaginal and lymphoid tissues were collected from euthanized animals, fixed and embedded in paraffin. *In situ* hybridization combined with immunohistochemical staining and immunochemistry were performed as described9, 12.

Digital atlases

Images of fields with SIV RNA+cells were acquired, merged (Photoshop 7.0 automerge), and, after using Photoshop Action procedures to delineate SIV RNA+cells, centroid X, Y

coordinates were assigned using MetaMorph software, and the coordinates were plotted with Excel.

Induction and measurement of MIP-3α and IL-8

HIV-1 ± GML was added to HVECs cultured as described25. Chemokines in the supernates were measured by ELISA25.

Microarray analysis

Gene expression profiles in cervix before and after intravaginal SIV inoculation were analysed with the AFFYMETRIX GeneChip® Rhesus Macaque Genome Array as described 26.

Statistical methods

The negative binomial distribution was used to model repeated challenges. The model assumes outcomes for distinct animals are independent and the probability of being infected differs between the 2 groups. Use of maximum likelihood or Bayesian methods (which don't assume the sample size is large) both indicate that GML's efficacy against transmission is at least 65%, where the posterior probability is 0.98 that GML is more likely to prevent infection than K-Y warming gel and the p-value is 0.04 that the probability differs between groups.

Methods

Animals

Adult female rhesus macaque monkeys (*Macacca mulatta*) used in the studies were housed at the California and Wisconsin National Primate Centers in accordance with the regulations of the American Association of Accreditation of Laboratory Animal Care and the standards of the Association for Assessment and Accreditation of Laboratory Animal Care International; all protocols and procedures were approved by the relevant Institutional Animal Care and Use Committee. All animals were negative for antibodies to HIV type 2, SIV, type D retrovirus, and simian T-cell lymphotropic virus type 1.

Intra-vaginal inoculation of SIV and GML and K-Y warming gel

Monkeys were inoculated intra-vaginally twice in a single day, with a 4-hour interval between inoculations, with one ml of a 2004 virus stock from Dr. C. Miller of 10^5 $TCID_{50}$/ml SIVmac 251. For inoculation, each animal was anesthetized with an intramuscular injection of a combination of ketamine hydrochloride (Parke-Davis, Morris Plains, NJ) (up to 7mg/kg) and medetomidine (up to 5 mg/kg). Additional ketamine, when needed, was given intravenously (up to 5 mg/kg). The animal was placed in a sternal position with her posterior elevated approximately 60 degrees from horizontal and a 1 ml syringe without a needle was inserted atraumatically into the vagina to deliver the inoculum. Animals thereafter remained in the sternal position for at least 30, but no more than 40 minutes. For GML 5% and vehicle control gel dosing, as well as collection of vaginal swabs, animals were transferred to a table-top restraint device to administer either 1 ml of

vehicle control K-Y warming gel or 1 ml of gel containing 50 mg solubilized GML via a 1 ml syringe without needle inserted atraumatically into the vagina, as described above.

GML formulation

GML (monomuls 90-L 12®, Cognis Corporation Care Chemicals, Cincinnati, Ohio) was dissolved in K-Y warming gel (5 gms/100 ml) at the Fairview Compounding Pharmacy, Minneapolis, MN.

Detection of SIV RNA in plasma

SIV viral RNA genomic copy equivalents in EDTA-anti-coagulated plasma was determined using a quantitative reverse-transcription PCR (qRT-PCR) procedure modified from an assay described previously24. Briefly, vRNA was isolated from plasma using a GuSCN-based procedure as described. QRT-PCR was performed using the SuperScript III Platinum(R) One-Step Quantitative RT-PCR System (Invitrogen, Carlsbad, CA). Reactions were run on a Roche Lightcycler 2.0 instrument and software. vRNA copy number was determined using LightCycler 4.0 software (Roche Molecular Diagnostics, Indianapolis, IN) to interpolate sample crossing points onto an internal standard curve prepared from 10-fold serial dilutions of a synthetic RNA transcript representing a conserved region of SIV gag.

Tissue collection and processing

At the time of euthanasia, blood, upper, middle and lower portions of vagina, cervix, and uterus, draining LNs (iliac, obturator and inguinal), mesenteric, axillary and inguinal LNs, gut (ileum, jejunum and colon) from each animal were collected, and fixed in 4% paraformaldehyde, SafeFix II (Fisher Scientific, Fairview, NJ) or Streck's fixative (Streck Laboratories, Inc., Omaha, NE), and embedded in paraffin for sectioning.

In situ hybridization (ISH)

In situ hybridization to detect SIV RNA was performed as previously described9. Briefly, After deparaffinization, pretreatment to permeabilize tissue and to block non-specific binding, 5 micron sections from 4% PFA fixed tissues were hybridized to ^{35}S-labeled SIV RNA antisense or sense (as a negative control) riboprobes covering over 90% of SIV genome; After overnight hybridization, the sections were washed, digested with ribonucleases, coated with nuclear track emulsion, exposed, developed, and counterstained with H &E.

Construction of digital atlas of SIV vRNA+cells in cervix and vagina

An image of each field with SIV RNA+cells detected by in situ hybridization was collected sequentially using epifluorescent illumination, Olympus B-MAX microscope (Olympus, Tokyo, Japan) and a "SPOT INSIGHT" digital camera (Diagnostic Instruments, Tokyo, Japan). The images from each section were acquired from left to right and top to bottom with a ~20% overlap with its neighboring images to avoid gaps in creating the montage image. Images were automatically merged into one Atlas image using a Photoshop 7.0 automerge function. After using the Photoshop Action procedures to associate individual silver grains with cells, the centroid X, Y coordinates of a SIV RNA+ cell were assigned

using MetaMorph (version 7.1.3.) software, and these coordinates were then logged into Excel files as numeric numbers and plotted with Excel.

Immunohistochemistry

Immunohistochemistry was performed as described9, 12 using a biotin-free detection system, MACH-3™ (Biocare Medical) or EnVision+ System (DakoCytomation), on 5 μm tissue sections mounted on glass slides. Tissues were deparaffinized and rehydrated in deionized water. Heat-induced epitope retrieval (HIER) was performed using the water bath method (95° to 98°C for 10–20 min) in one of the following buffers: 1X EDTA Decloaker™ reagent (Biocare Medical), 1X DiVA Decloaker (Biocare Medical), 10mm/L sodium citrate, pH 6.0, or 1mm EDTA, pH 8.0, followed by cooling to room temperature. Tissues sections were blocked with SNIPER Blocking Reagent (Biocare Medical) for 1h at room temperature. Endogenous peroxidase was blocked with 3% (v/v) H2O2 in TBS (pH 7.4). Primary antibodies were diluted in 10% SNIPER Blocking Reagent in TNB and incubated overnight at 4°C. Following the primary antibody incubation, the sections were washed and then incubated with either mouse, goat or rabbit polymer system reagents conjugated with either horseradish peroxidase or alkaline phosphatase according to the manufacturer's instructions and developed with 3,3′-diaminobenzidine (Vector Laboratories, Burlingame, CA) or Vulcan Fast Red (Biocare Medical). Sections were counterstained with CAT Hematoxylin (Biocare Medical), mounted in Permount (Fisher Scientific) and examined by light microscopy. Primary antibodies and other reagents and protocols used are summarized in End notes. All anti-human antibody reagents were demonstrated to show good cross reactivity with the cognate macaque antigens. Isotype matched IgG negative control antibodies in all instances yielded negative staining results.

Immunohistochemical staining (IHCS) and in situ hybridization (ISH)

Combined IHCS and ISH were performed as described previously9. In brief, sections were microwaved for antigen retrieval, hybridized, washed and digested with ribonucleases, incubated with antibody markers for cell type, CD3, CD4, CD68, and then stained with the Dako Envision + Peroxidase kit with antibodies to the primary antibody and diaminobenzidine (DAB). After washing, the sections were coated with nuclear track emulsion, exposed, developed, and counterstained with hematoxylin.

Culture of HVECs and induction and measurement of MIP-3α and IL-8

HVECs were cultured until confluent at 37°C, 7% CO2 in 96-well flat-bottom microtiter plates (Becton Dickinson Labware, Franklin Lakes, NJ) in 100 μl per well of keratinocyte serum free medium (KSFM) with antibiotics 25. HIV-1 ± GML was added to wells, and, after 6 hours incubation, supernates were collected and tested for chemokines by ELISA as described by the manufacturer (R&D Systems, Minneapolis, MN). Data reported are mean ± standard deviation. We have previously shown25 that GML does not interfere with ELISA for chemokine detection.

Microarray analysis of cervical transcriptional responses to intravaginal SIV inoculation

Gene expression profiles in cervix of macaques before and after intravaginal SIV inoculation at 1 and 3 dpi were analysed with the GeneChip® Rhesus Macaque Genome Array (AFFYMETRIX, INC. 3380 Central Expressway, Santa Clara, CA 95051 USA), which contains ~ 47,000 rhesus transcripts. RNA extractions, preparation of biotin-labeled cRNA probes, and microarray hybridization followed previously published protocols26. Briefly, snap-frozen cervical tissues from two un-infected and three infected Indian rhesus macaques at 1 dpi and two macaques at 3 dpi were homogenized, total RNA was extracted, double-stranded cDNA and biotin-labeled cRNA probes were synthesized from 5 μg of total RNA. Fifteen micrograms of fragmented cRNA was hybridized to an Affymetrix the GeneChip® Rhesus Macaque Genome Array. After hybridization, chips were washed, stained with streptavidin-phycoerythrin, and scanned with GeneChip Operating Software at the Biomedical Genomics Center at the University of Minnesota. The experiments from each RNA sample were duplicated in the preparation of each cRNA probe, and microarray hybridization. Microarray data were analyzed in Expressionist program Genedata, Pro version 4.5, using the RMA algorithm. The expression levels from duplicated chips of the same animals' RNA were correlated and averaged. Tests for differences between the uninfected and infected animals at 1dpi and 3 dpi were conducted using the 2-sample t-test. Cut-off was set at $p < 0.05$ and ≥ 2-fold increased expression.

Statistical methods

In the initial protocol, animals were challenged twice and then necropsied at peak replication in order to obtain tissues to evaluate viral replication, whereas, in the second experiment, each animal was repeatedly challenged until all of the controls were infected. For this second experiment, we used the negative binomial likelihood as a statistical model to interpret the results of the experiment. Note that since the design of the second stage of the experiment included the possibility that treated animals would never get infected, animals in the treatment group who were not infected were considered to be right censored at the trial at which all the controls were finally infected. Since the challenge involved 2 doses at each time point, our trials consist of 2 such doses. So an animal that survived 2 challenges was subjected to 4 doses. Our model supposes that a success for a trial occurs when an animal is infected by one of these double dose challenges. Moreover, the model supposes that the outcome for each animal is independent and there is a different probability of a success for a trial depending on treatment status. Hence, if we let θ represent the probability that an animal is infected with one challenge, and an animal is infected on the m^{th} challenge, then this animal contributes a factor of $(1-\theta)^{m-}1\theta$ to the likelihood. For an animal that survives m such challenges, then since the probability that this occurs is $(1-\theta)^m$, this animal would contribute $(1-\theta)^m$ to the likelihood. The likelihood for each group is then found by multiplying the contributions from each animal The likelihood in that group. Maximum likelihood estimates are then found by maximizing the likelihood. We can also compute Bayesian credible sets and the posterior probability that the probability of success differs between the 2 groups using numerical integration (using an adaptive 15-point Gauss-Kronrod quadrature, as implemented in the software S-plus, version 3.4 release 1, from Mathsoft, Inc.). For the groups of three animals challenged four times, GML's efficacy

against transmission is estimated to be at least 65%, and the probability that GML is more likely to prevent infection than K-Y warming gel alone is 0.98. While we prefer this estimate, because the outcome was determined decisively, including the animals in the pilot experiment where we did not repeatedly challenge until infected, 5/5 GML treated animals and 1/5 controls did not get infected. The estimated efficacy of GML (using the same methods) in this case is at least 72% at a probability of 0.95.

Supplementary Material

Refer to Web version on PubMed Central for supplementary material.

Acknowledgments

The authors thank Chris Miller and Ding Lu at the California National Primate Research Center, University of California at Davis, for helpful discussion and virus stocks, Joseph Kemnitz at the Wisconsin National Primate Research Center, University of Wisconsin at Madison, for helpful discussion and administrative support, and Colleen O'Neill and Tim Leonard for help with the manuscript and figures. This work was supported in part by National Institute of Health (N.I.H.) grants R21 AI071976 and P01 AI066314 (A.T.H.), funds from the National Cancer Institute, N.I.H., under contracts N01-CO-12400 and HHSN266200400088C (J.D.L.), and Grant Number P51 RR000167 from the National Center for Research Resources (NCRR), a component of the N.I.H., to the Wisconsin National Primate Research Center. This research was conducted in part at a facility constructed with support from Research Facilities Improvement Program grant numbers RR15459-01 and RR020141-01. This publication's contents are solely the responsibility of the authors and do not necessarily represent the official views of the NCRR or NIH.

References

1. Fauci AS. 25 years of HIV. Nature. 2008; 453:289–290. [PubMed: 18480799]
2. Ledford H. HIV vaccine may raise risk. Nature. 2007; 450:325. [PubMed: 18004331]
3. Check E. Scientists rethink approach to HIV gels. Nature. 2007; 446:12.
4. Cohen J. AIDS research. Microbicide fails to protect against HIV. Science. 2008; 319:1026–1027. [PubMed: 18292313]
5. Haase AT. Perils at mucosal front lines for HIV and SIV and their hosts. Nat Rev Immunol. 2005; 5:783–792. [PubMed: 16200081]
6. Miller CJ, et al. Propagation and dissemination of infection after vaginal transmission of SIV. J Virol. 2005; 79:9217–9227. [PubMed: 15994816]
7. Kabara, JJ. Cosmetic and Drug Preservation. Marcel Dekker, Inc; New York: 1984. Fatty acids and derivatives as antimicrobial agents: a review.
8. Peterson ML, Schlievert PM. Glycerol monolaurate inhibits the effects of Gram-positive select agents on eukaryotic cells. Biochemistry. 2006; 45:2387–97. [PubMed: 16475828]
9. Li Q, et al. Peak SIV replication in resting memory CD4(+) T cells depletes gut lamina propria CD4(+) T cells. Nature. 2005; 434:1148–1152. [PubMed: 15793562]
10. Mattapallil JJ, et al. Massive infection and loss of memory CD4(+) T cells in multiple tissues during acute SIV infection. Nature. 2005; 434:1093–1097. [PubMed: 15793563]
11. Colonna M, Trinchieri G, Liu YJ. Plasmacytoid dendritic cells in immunity. Nat Immunol. 2004; 5:1219–1226. [PubMed: 15549123]
12. Estes JD, et al. Premature induction of an immunosuppressive regulatory T cell response during acute simian immunodeficiency virus infection. J Infect Dis. 2006; 193:703–712. [PubMed: 16453267]
13. Dieu-Nosjean MC, Vicari A, Lebecque S, Caux C. Regulation of dendritic cell trafficking: a process that involves the participation of selective chemokines. J Leukoc Biol. 1999; 66:252–262. [PubMed: 10449163]

14. Schlievert PM JR, Deringer MH, Kim SJ, Projan, Novick RP. Effect of glycerol monolaurate on bacterial growth and toxin production. Antimicrob Agents Chemother. 1992; 36:626–632. [PubMed: 1622174]
15. Narimatsu R, Wolday D, Patterson BK. IL-8 increases transmission of HIV type 1 in cervical explant tissue. AIDS Res Hum Retroviruses. 2005; 21:228–233. [PubMed: 15795529]
16. Schlievert PM, et al. Glycerol monolaurate does not alter rhesus macaque (Macaca mulata) vaginal lactobacilli and is safe for chronic use. Antimicrob Agents Chemother. 2008 In press.
17. Crane-Godreau MA, Wira CR. CCL20/macrophage inflammatory protein 3alpha and tumor necrosis factor alpha production by primary uterine epithelial cells in response to treatment with lipopolysaccharide or Pam3Cys. Infect Immun. 2005; 73:476–484. [PubMed: 15618187]
18. Wira CR, Fahey JV, Sentman CL, Pioli PA, Shen L. Innate and adaptive immunity in female genital tract: cellular responses and interactions. Immunol Rev. 2005; 206:306–335. [PubMed: 16048557]
19. Wang Y, et al. The Toll-like receptor 7 (TLR7) agonist, imiquimod, and the TLR9 agonist, CpG ODN, induce antiviral cytokines and chemokines but do not prevent vaginal transmission of simian immunodeficiency virus when applied intravaginally to rhesus macaques. J Virol. 2005; 79:14355–14370. [PubMed: 16254370]
20. Klasse PJ, Shattock RJ, Moore JP. Which topical microbicides for blocking HIV-1 transmission will work in the real world? PLoS Med. 2006; 3:e351. [PubMed: 16903780]
21. Ma, Zhong-Min; Abel, Kristina; Rourke, Tracy; Wang, Yichuan; Miller, Christopher J. A Period of Transient Viremia and Occult Infection Precedes Persistent Viremia and Antiviral Immune Responses during Multiple Low-Dose Intravaginal Simian Immunode ciency Virus Inoculations. J Virol. 2004; 78:14048–14052. [PubMed: 15564513]
22. Johnston R. Microbicides 2002: an update. AIDS Patient Care STDS. 2002; 16(9):419–30. [PubMed: 12396694]
23. Shattock RJ, Moore JP. Inhibiting sexual transmission of HIV-1 infection. Nat Rev Microbiol. 2003; 1:25–34. [PubMed: 15040177]
24. Cline AN, Bess JW, Piatak M Jr, Lifson JD. Highly sensitive SIV plasma viral load assay: practical considerations, realistic performance expectations, and application to reverse engineering of vaccines for AIDS. J Med Primatol. 2005; 34:303–31236. [PubMed: 16128925]
25. Peterson ML, et al. The innate immune system is activated by stimulation of vaginal epithelial cells with *Staphylococcus aureus* and toxic shock syndrome toxin 1. Infect Immun. 2005; 73:2164–2174. [PubMed: 15784559]
26. Li Q, et al. Functional genomic analysis of the response of HIV-1 infected lymphatic tissue to antiretroviral therapy. J Infect Dis. 2004; 189:572–582. [PubMed: 14767808]

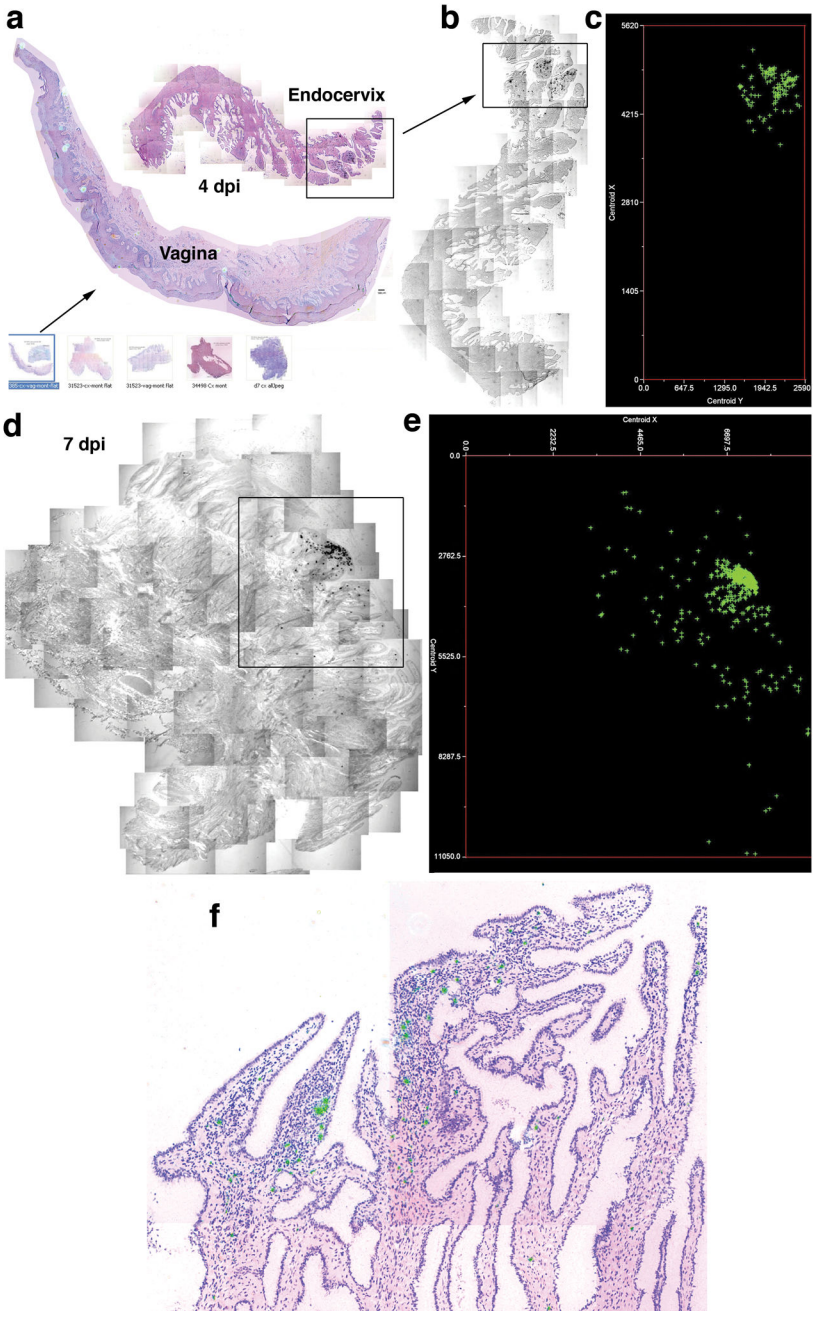

Figure 1.

Mapping early expansion of infection in endocervix. SIV RNA+ cells appear black in transmitted light, green in reflected light and in maps. a–c. The arrow from thumbnail montage images (bottom of 1a) of cervix and vagina, 4–10dpi, points to an enlarged image and map of a single focus (box) of SIV RNA+ cells in endocervix, 4dpi. Counter clockwise-rotated image of focus (box) and map of X, Y coordinates (μm) of cell centroids to the right. d–e. Endocervical focus and map, 7dpi. f. Endocervical focus, 6dpi, SIV RNA+ cells (green) are concentrated in an inflammatory infiltrate (cells with dark staining nuclei).

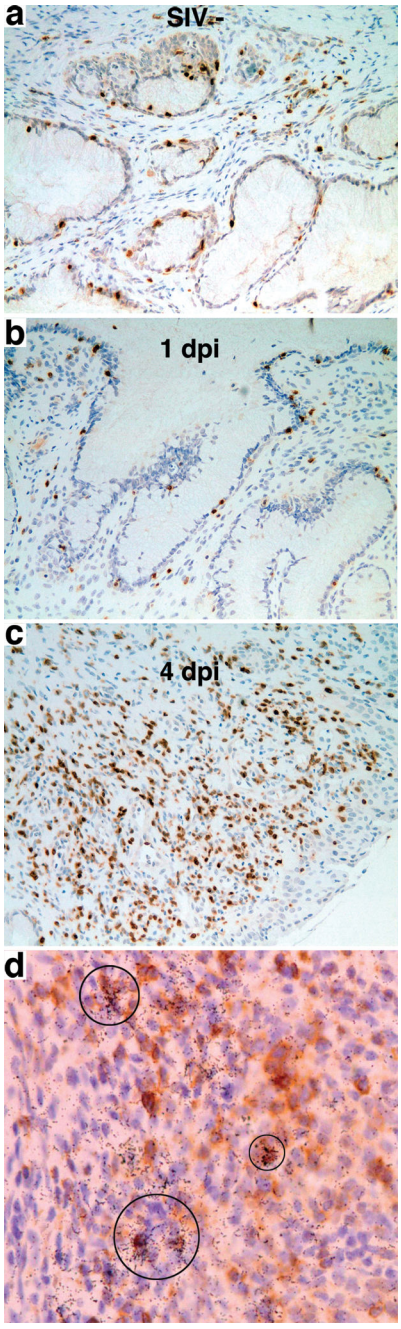

Figure 2.

Influx and infection of CD4+ T cells in cervix in early infection. a–c. Sections stained with anti-CD4. Note relative paucity of CD4+ cells in SIV-(negative animal) (a), or SIV inoculated animal 1 dpi (b), compared to increased numbers of CD4+ cells seen in infected animal at 4 dpi (c). d. SIV RNA+ cells in infiltrates are CD3+ T cells. Encircled SIV RNA+ cells (overlying black silver grains) are stained brown with anti-CD3.

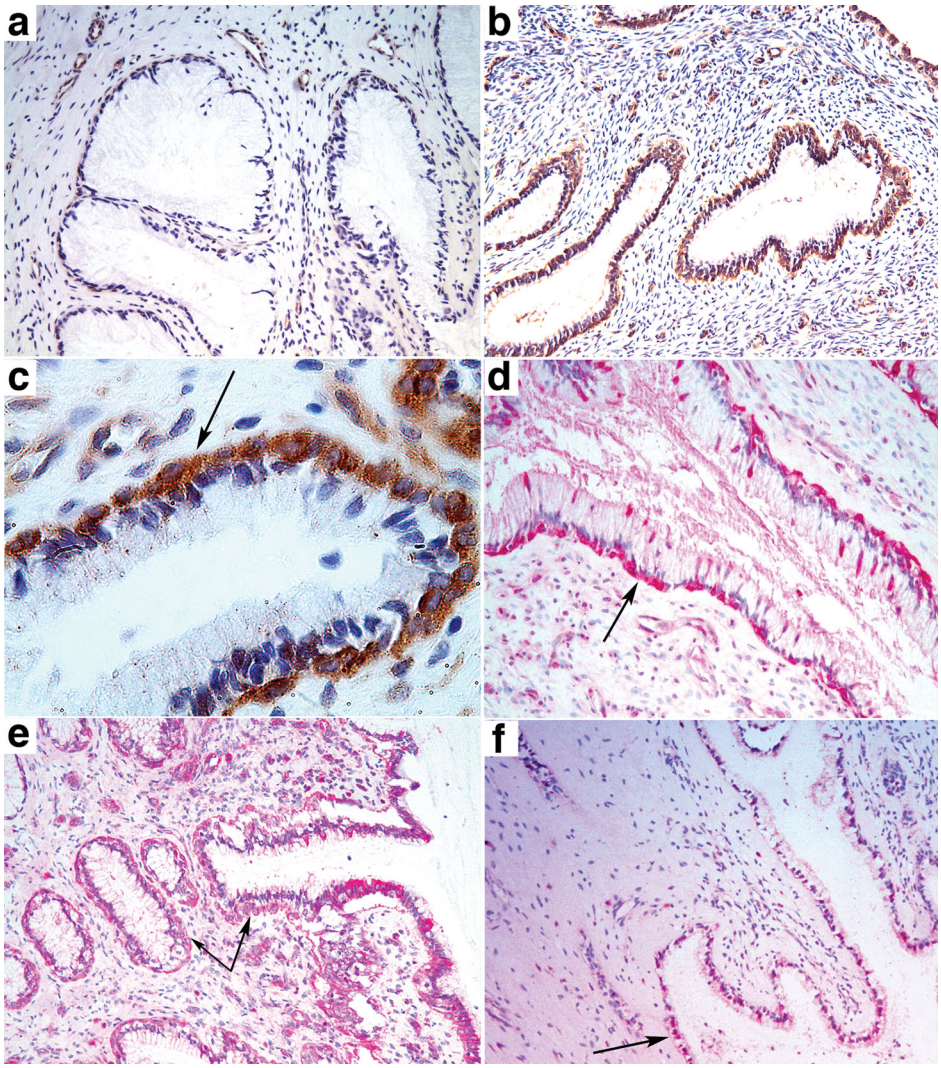

Figure 3.

pDCs, cytokines and chemokines associated with endocervical epithelium following exposure to SIV. a. Uninfected animal. b–c. Rapid accumulation of pDCs beneath endocervical epithelium at 1 dpi shown at 10X (b) and 40X (c) original magnifications. pDCs stained brown with anti-CD123. Arrow in c points to the location of pDCs beneath the epithelium. d–e. Arrows point to subepithelial pDCs stained red with anti-interferon-α at 1 dpi (d) or anti-MIP-1β (e). f. Arrow points to MIP-3α+ endocervical epithelium (red) at 1 dpi.

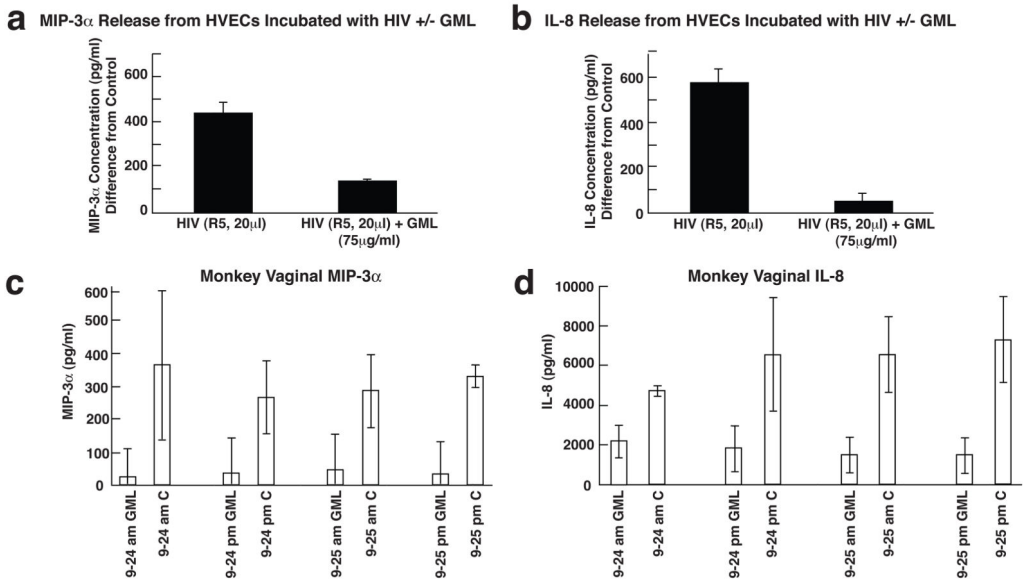

Figure 4.

GML inhibits HIV-1 induced expression of MIP-3α and IL-8 in HVECs and in cervical vaginal fluids. a–b. R5 isolate of HIV-1 added to HVECs in the amounts indicated± GML. c–d. At the end of a six-month safety study, cervical vaginal fluids were collected with a swab that reproducibly adsorbed 0.1 ml of fluid from animals that received GML or K-Y warming gel in the am and pm on two successive days. MIP-3α and IL-8 measured by ELISA. Bars indicate standard errors of the mean.

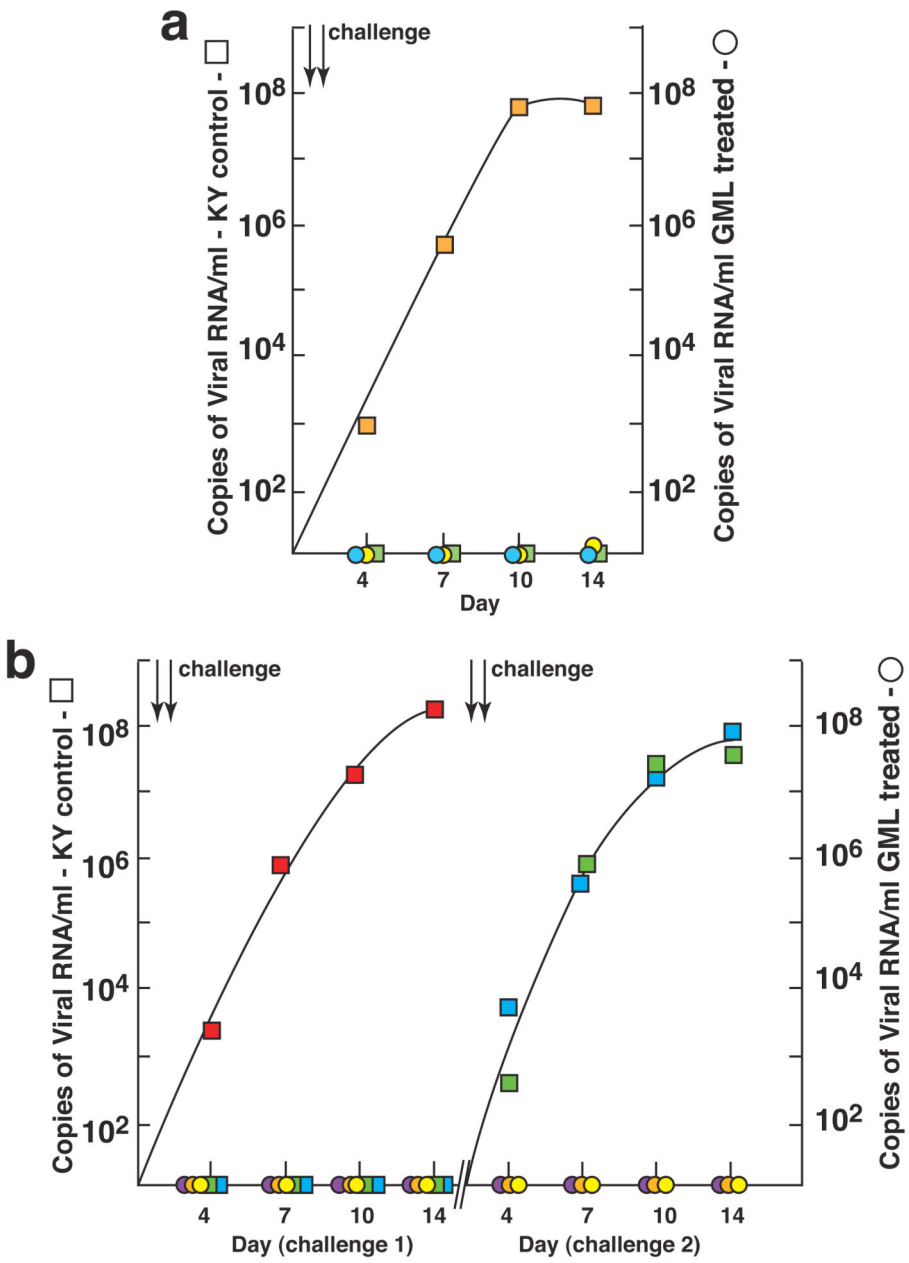

Figure 5.

GML prevents mucosal transmission and acute infection. a. Pilot experiment continuation of daily dosing safety study. Two animals treated with GML in K-Y warming gel (circles) and two treated with gel only (squares) were challenged twice (two arrows), 1-hour after treatment, with 10^5 $TCID_{50}$ of SIV. Colors indicate individual animals. SIV RNA in plasma was measured to peak viremia, 14 dpi. b. Three animals treated with GML and three given K-Y warming gel were challenged as described in a. The animals that were not infected were treated and challenged again 4 weeks later, shown at the right.

Immunohistochemical staining, protocols and reagents

Antibody/Reagent	Clone/ catalog no.	Tissue fixation	Antigen-retrieval pre-treatment	Antibody Dilution	Manufacturer	Address
CCL3/MIP-1α	RB-10489-P	4% PFA (paraformaldehyde)	Diva Decloaker water bath for 20 min at 95°C–98°C	1:100	Lab Vision/NeoMarkers	47790 Westinghouse Dr. Fremont, CA 94539
CCL4/MIP-1β	AF-271-NA	4% PFA	Diva Decloaker water bath for 20 min at 95°C–98°C	1:100	R&D Systems	614 McKinley Place NE Minneapolis, MN 55413
CCL5/RANTES	AF-278-NA	4% PFA	Diva Decloaker water bath for 20 min at 95°C–98°C	1:50	R&D Systems	614 McKinley Place NE Minneapolis, MN 55413
CCL20/MIP-3α	206D9.05	SF Streck's fixative	Decloaker water bath for 20 min at 95°C–98°C	1:50	Dendritics	Bioparc Laennec 60 Avenue Rockefeller-69008 LYON France
CCL20/MIP-3α	319F6.06	SF	Decloaker water bath for 20 min at 95°C–98°C	1:50	Dendritics	Bioparc Laennec 60 Avenue Rockefeller-69008 LYON France
CD123/IL-3Rα	SC-681	4% PFA & SF	Diva Decloaker water bath for 20 min at 95°C–98°C	1:500–2000	Santa Cruz Biotechnology Inc.	San Jose, CA 95131-1807
CD3	SP7	4% PFA	10 mmol/L sodium citrate, pH 6.0; water bath for 15 min at 95°C–98°C	1:100	*Lab Vision/NeoMarkers*	47790 Westinghouse Dr. Fremont, CA 94539
CD3	F7.2.38,	4% PFA	Diva Decloaker water bath for 20 min at 95°C–98°C	1:100	DakoCytomation	6392 Via Real, Carpinteria, CA 93013
CD4	IF6	4% PFA	1 mmol/L EDTA, pH 8.0; water bath for 10 min at 95°C–98°C	1:5–1:25	Novocastra Laboratories Ltd	Balliol Business Park West, Benton Lane, Newcastle upon Tyne, NE12 8EW, UK
CD68	KP1	4% PFA & SF	10 mmol/L sodium citrate, pH 6.0; water bath for 15 min at 95°C–98°C	1:200	Dako Cytomation	6392 Via Real, Carpinteria, CA 93013
IL-8	Ab9630	4% PFA & *SF*	10 mmol/L sodium citrate, pH 6.0; high pressure cooker (Pascal Dako Corp.) for 3 min at 120°C	1:50–100	Abcam Inc.	1 Kendall Square, Ste 341 Cambridge, MA 02139-1517
BDCA-2	104C12.08	SF	Decloaker water bath for 20 min at 95°C–98°C	1:100	Dendritics	Bioparc Laennec 60 Avenue Rockefeller-69008 LYON France
Interferon-alpha	MMHB-2	4% PFA	Diva Decloaker water bath for 20 min at 95°C–98°C	1:200	Calbiochem	10394 Pacific Ctr. Ct. San Diego, CA 92121
Interferon-beta	MMHB-16	4% PFA	Diva Decloaker water bath for 20 min at 95°C–98°C	1:200	PBL Biomedical Laboratories	100 Jersey Avenue, Building D New Brunswick, NJ 08901

Antibody/Reagent	Clone/ catalog no.	Tissue fixation	Antigen-retrieval pre-treatment	Antibody Dilution	Manufacturer	Address
Goat ChromPure IgG (Isotype control)	011-000-003	4% PFA & SF	Diva Decloaker water bath for 20 min at 95°C–98°C	1:50–1:100	Jackson Immuno-Research	P.O. Box 9 872 West Baltimore Pike West Grove, PA 19390
Mouse IgG1 (Isotype control)	X 0931	4% PFA & SF	Diva Decloaker water bath for 20 min at 95°C–98°C	1:25–1:200	Dako Cytomation	6392 Via Real, Carpinteria, CA 93013
Mouse IgG2a (Isotype control)	X 0943	4% PFA & SF	Diva Decloaker water bath for 20 min at 95°C–98°C	1:25–1:200	Dako Cytomation	6392 Via Real, Carpinteria, CA 93013
Rabbit ChromPure IgG (Isotype control)	005-000-003	4% PFA & SF	Diva Decloaker water bath for 20 min at 95°C–98°C	1:500–2000	Jackson Immuno-Research	P.O. Box 9 872 West Baltimore Pike West Grove, PA 19390